

# ON PRECONDITIONING SADDLE POINT SYSTEMS WITH TRACE CONSTRAINTS COUPLING 3D AND 1D DOMAINS – APPLICATIONS TO MATCHING AND NONMATCHING FEM DISCRETIZATIONS \*

MIROSLAV KUČHTA <sup>†</sup>, KENT-ANDRE MARDAL <sup>†‡</sup>, AND MIKAEL MORTENSEN <sup>†</sup>

**Abstract.** Multiscale or multiphysics problems often involve the coupling of partial differential equations posed on domains of different dimensionality. In this work we consider a simplified model problem of a 3d-1d coupling and the main motivation is to construct algorithms that may utilize standard multilevel algorithms for the 3d domain, which has the dominating computational complexity. Preconditioning for a system of two elliptic problems posed, respectively, in a three dimensional domain and an embedded one dimensional curve and coupled by the trace constraint is discussed. Investigating numerically the properties of the well-defined discrete trace operator, it is found that negative fractional Sobolev norms are suitable preconditioners for the Schur complement. The norms are employed to construct a robust block diagonal preconditioner for the coupled problem.

**Key words.** preconditioning, saddle-point problem, Lagrange multipliers, trace

**AMS subject classifications.** 65F08

**1. Introduction.** Let  $\Omega$  be a bounded domain in  $3d$ , while  $\Gamma$  represents a  $1d$  structure inside  $\Omega$ , and consider the following coupled problem

$$-\Delta u + u + p\delta_\Gamma = f \quad \text{in } \Omega, \quad (1.1a)$$

$$-\Delta v + v - p = g \quad \text{on } \Gamma, \quad (1.1b)$$

$$Tu - v = h \quad \text{on } \Gamma. \quad (1.1c)$$

Here the term  $p\delta_\Gamma$  is to be understood as a Dirac measure such that  $\int_\Omega p(x)\delta_\Gamma v(x) dx = \int_\Gamma p(t)v(t) dt$  for a continuous function  $v$ . We remark that from a mathematical point of view the trace  $T$  of  $u$  required in (1.1c) is in the continuous case not well-defined unless the functions are sufficiently regular. For simplicity, the system shall be considered with homogeneous Neumann boundary conditions.

The system (1.1) is relevant in numerous biological applications where the embedded (three dimensional) structure is such that order reduction techniques can be used to capture its response by a one dimensional model. Equation (1.1a) then models processes in the bulk, while (1.1c) is the coupling between the domains. A typical example of such a system is a vascular network surrounded by a tissue and the order reduction is due to assumption of radii of the arteries being negligible in comparison to their lengths. To list a few concrete applications, the 3d-1d models have been used, e.g., in [17, 21, 16, 31] to study blood and oxygen transport in the brain or in [11] to describe fluid exchange between microcirculation and tissue interstitium. Efficiency of cancer therapies delivered through microcirculation was studied in [10], and hyperthermia as a cancer treatment in [27]. We note that the employed models are more involved than (1.1), but that the system still qualifies as a relevant model problem.

---

<sup>†</sup>Department of Mathematics, Division of Mechanics, University of Oslo {mirok, mikaem}@math.uio.no

<sup>‡</sup>Center for Biomedical Computing, Simula Research Laboratory, kent-and@simula.no

\* The work of Kent-Andre Mardal and Mikael Mortensen has been supported by a Center of Excellence grant no. 179578 from the Research Council of Norway to the Center for Biomedical Computing at Simula Research Laboratory. The work of Kent-Andre Mardal has also been supported by the Research Council of Norway through grant no. 209951.

Due to the measure term and the three-to-one dimensional trace operator, the problem (1.1) is not standard and establishing its well-posedness is a delicate issue. In fact, considering (1.1a) with a known  $p$  and homogeneous Dirichlet boundary conditions, the equation is not solvable in  $H_0^1(\Omega)$ , as  $\nabla u$  may be unbounded in the neighborhood of  $\Gamma$ . A similar problem was studied in [14], where two elliptic problems were coupled via a measure source term, and a unique weak solution was found using weighted Sobolev spaces. In particular, the weighted spaces ensured that the trace could be defined as a bounded operator. A corresponding finite element method (FEM) for the problem was discussed in [13], where optimal convergence in the weighted Sobolev norm was shown using graded meshes. For an elliptic problem with measure data, it was shown in [19] that FEM with regular meshes yields optimal convergence in the  $L^2$  norm outside of the fixed neighborhood of the singularity. We note that the more application oriented works [11, 10, 27], that build on the analysis in [14, 13], relied on incomplete LU preconditioning.

In the current paper we shall *assume* that (1.1) is well posed and the focus is then on the construction of optimal preconditioners for the linear system due to (1.1) and FEM. Because the computational complexity of the 3d problem dominates the 1d problem, we put focus on preconditioners that are composed of standard multilevel algorithms for the 3d problem. This means that the weighted Sobolev spaces, or extra regularity in the equation in the 3d domain (1.1a), is disregarded, and that we rather add an extra requirement to (1.1c). We note that  $u$  shall be approximated within  $H^1$  conforming finite element spaces and as such the approximation has a well defined trace.

The current paper is an extension of [20], where a system similar to (1.1a)–(1.1c) was analyzed for the case  $\Omega$  a bounded domain in  $2d$  and  $\Gamma$  a structure of codimension one. Therein, robust preconditioners were established, based on the operator preconditioning framework [26], in which preconditioners are constructed as approximate Riesz mappings in properly chosen Hilbert spaces. The framework often allows for construction of order-optimal preconditioners, with convergence independent of material and discretization parameters, directly from the analysis of the continuous system of equations. In particular, in [20] it was shown that the proper preconditioning relied on a nonstandard fractional  $H^{\frac{1}{2}}$  inner product. Crucial for the analysis was the fact that the trace operator  $T$  is a well-defined mapping between  $H^1(\Omega)$  and  $H^{\frac{1}{2}}(\Gamma)$ , when  $\Gamma$  is of codimension one with respect to  $\Omega$ . Furthermore, for the finite element approximation in [20], it was assumed that the discrete meshes representing  $\Gamma$  and  $\Omega$  *matched* in the sense that the cells of the mesh of  $\Gamma$  were edges in the mesh of  $\Omega$ . Finally, only continuous linear Lagrange elements were used.

This paper utilizes ideas presented in [20] for the construction of the preconditioner, but here we go beyond what was theoretically established. In particular, we consider the case where  $\Gamma$  is of codimension two with respect to  $\Omega$ . As the trace operator  $T$  is not well-defined in the continuous case, we do not attempt to provide mathematically rigorous proofs, as this would require additional regularity of the solution. Instead, we study for which  $s$  the  $H^s$  inner product provides numerically stable behaviour. In addition, we consider the case where the discretizations of  $\Gamma$  and  $\Omega$  do not match. Finally, an approximation by discontinuous elements is discussed.

Our work is structured as follows. In §2 the theoretical background is presented. Section 3 discusses numerical experiments using spectral and finite element discretizations that identify suitable norms for the discrete 3d-1d trace operator. In §4 the identified norms are employed to construct optimal preconditioners for coupled model

3d-1d problems discretized with FEM and matched discretizations of  $\Omega$  and  $\Gamma$ . In §5 this restriction is lifted, the corresponding inf-sup condition is discussed, and we present numerical experiments that suggest the identified norms lead to good preconditioners. Finally, conclusions are drawn in §6.

**2. Notation and preliminaries.** Let  $X$  be a Hilbert space of functions defined on a domain  $D \subset \mathbb{R}^d$ ,  $d = 1, 2, 3$ . The norm of the space is denoted by  $\|\cdot\|_X$ , while  $\langle \cdot, \cdot \rangle_{X', X}$  is the duality pairing between  $X$  and its dual space  $X'$ . We let  $(\cdot, \cdot)_X$  denote the inner product of  $X$ , while, to simplify the notation,  $(\cdot, \cdot)_D$  is the  $L^2$  inner product. The Sobolev space of functions with  $m$  square integrable derivatives is  $H^m(D)$ . Finally,  $H_0^m(D)$  denotes the closure of the space of smooth functions with compact support in  $D$  in the  $H^m(D)$  norm.

We use normal capital font to denote operators over infinite dimensional spaces, e.g.  $A : X \rightarrow X'$ . For a discrete subspace  $X_h \subset X$ ,  $\dim X_h = n$ , the subscript  $h$  is used to distinguish the finite dimensional operator due to the Galerkin method, e.g.,  $A_h : X_h \rightarrow X_h'$  defined by

$$\langle A_h u_h, v_h \rangle_{X', X} = \langle Au, v_h \rangle_{X', X} \quad u_h, v_h \in X_h \text{ and } u \in X.$$

For a given basis,  $\{\phi_i\}_{i=1}^n$  of  $X_h$ , the matrix representation of the operator is denoted by sans serif font. Thus  $A_h$  is represented by  $\mathbf{A} \in \mathbb{R}^{n \times n}$  with entries

$$\mathbf{A}_{i,j} = \langle A_h \phi_j, \phi_i \rangle_{X', X}.$$

Finally, the function  $u_h \in X_h$  is represented in the basis by a coefficient vector  $\mathbf{u} \in \mathbb{R}^n$ , where  $u_h = \mathbf{u}_i \phi_i$  (summation convention invoked).

**2.1. Properties of the trace operator.** We consider  $\Omega \subset \mathbb{R}^d$  an open connected domain with Lipschitz boundary  $\partial\Omega$  and  $\Gamma$  a Lipschitz submanifold of codimension one or two in  $\Omega$ . The trace operator  $T$  is defined by  $Tu = u|_\Gamma$  for  $u \in C(\overline{\Omega})$ .

In case the codimension of  $\Gamma$  is one, the properties of the trace operator are well known. In particular,  $T : H^1(\Omega) \rightarrow H^{\frac{1}{2}}(\Gamma)$  is bounded and surjective, see, e.g., [1, ch. 7], where  $H^{\frac{1}{2}}(\Gamma)$  is a fractional Sobolev space equipped with the norm

$$\|u\|_{H^{\frac{1}{2}}(\Gamma)}^2 = \|u\|_{L^2(\Gamma)}^2 + \int_{\Gamma \times \Gamma} \frac{|u(x) - u(y)|^2}{|x - y|^{d+1}} dx dy.$$

Moreover,  $T : H_0^1(\Omega) \rightarrow H^{\frac{1}{2}}(\Gamma)$  is bounded, but not surjective. To define the trace over  $H_0^1(\Omega)$  as a surjective operator, the range is given as  $H_{00}^{\frac{1}{2}}(\Gamma)$ ,

$$H_{00}^{\frac{1}{2}}(\Gamma) = \{u \in H^{\frac{1}{2}}(\Gamma); \tilde{u} \in H^{\frac{1}{2}}(\tilde{\Gamma})\} \text{ where } \tilde{u}(x) = \begin{cases} u(x) & x \in \Gamma \\ 0 & x \in \tilde{\Gamma} \setminus \Gamma \end{cases}$$

and  $\tilde{\Gamma}$  is some suitable extension of  $\Gamma$ , e.g.,  $\tilde{\Gamma} = \Gamma \cup \partial\Omega$ , in which case  $\|u\|_{H_{00}^{\frac{1}{2}}(\Gamma)} = \|\tilde{u}\|_{H^{\frac{1}{2}}(\tilde{\Gamma})}$ . We refer to [20] for these results.

The integral norms of  $H^{\frac{1}{2}}(\Gamma)$  and  $H_{00}^{\frac{1}{2}}(\Gamma)$  can be expensive to compute. For construction of efficient numerical algorithms, it is therefore more suitable to relate the spaces to interpolation spaces, see [22, 5] or [20]. For the sake of completeness, we review here the presentation from [20]. Let  $u, v \in X = H^1(\Gamma)$ . For  $u$  fixed  $v \mapsto (u, v)_\Gamma$  is in  $X'$  and by the Riesz-Fréchet theorem there is a unique  $w \in X$  such that  $(w, v)_X = (u, v)_\Gamma$  for any  $v \in X$ . The operator  $S : u \rightarrow w$  is injective and compact

and thus the eigenvalue problem  $S\phi_i = \lambda_i\phi_i$  (no summation implied) is well-defined. In addition,  $S$  is self-adjoint and positive-definite such that the eigenvalues form a nonincreasing sequence  $0 < \lambda_{k+1} \leq \lambda_k$  and  $\lambda_k \rightarrow 0$ . By definition, the eigenvectors satisfy

$$(\phi_i, v)_X = \lambda_i^{-1}(\phi_i, v)_\Gamma \quad v \in X,$$

or equivalently

$$A\phi_i = \lambda_i^{-1}M\phi_i \text{ with } \langle Au, v \rangle_{X',X} = (u, v)_X \text{ and } \langle Mu, v \rangle_{X',X} = (u, v)_\Gamma. \quad (2.1)$$

Further, the set of eigenvectors  $\{\phi_k\}_{k=1}^\infty$  forms a basis of  $X$ , which is orthogonal in the inner product of  $X$  and orthonormal in the  $L^2(\Gamma)$  inner product. Finally, for  $s \in [-1, 1]$  we define the  $s$ -norm of  $u = c_k\phi_k \in \text{span}\{\phi_k\}_{k=1}^\infty$  as

$$\|u\|_{H_s(\Gamma)} = \sqrt{c_k^2 \lambda_k^{-s}}. \quad (2.2)$$

The space  $H_s(\Gamma)$  is defined as the closure of the  $\text{span}\{\phi_k\}_{k=1}^\infty$  in the  $s$ -norm, while  $H_{s,0}(\Gamma)$  is then defined analogically to  $H^s(\Gamma)$  with  $X = H_0^1(\Gamma)$  in the construction. We remark that  $H_0(\Gamma) = L^2(\Gamma)$ ,  $H_{1,0} = H_0^1(\Gamma)$ ,  $H_1 = H^1(\Gamma)$  and the norms of the spaces are equal. Moreover  $H_{\frac{1}{2}}(\Gamma) = H^{\frac{1}{2}}(\Gamma)$  and  $H_{\frac{1}{2},0}(\Gamma) = H_{00}^{\frac{1}{2}}(\Gamma)$  with the equivalence of norms.

Following the approach in [20], a weak formulation of the homogeneous Dirichlet problem for (1.1)–(1.1c) with  $\Omega \in \mathbb{R}^3$ ,  $\Gamma \subset \Omega$  of codimension one, using the method of Lagrange multipliers, reads: Find  $(u, v, p) \in H_0^1(\Omega) \times H_0^1(\Gamma) \times Q$  such that

$$\begin{aligned} (\nabla u, \nabla \phi)_\Omega + (u, \phi)_\Omega + (p, T\phi)_\Gamma &= (f, \phi)_\Omega & \phi &\in H_0^1(\Omega), \\ (\nabla v, \nabla \psi)_\Gamma + (v, \psi)_\Gamma - (p, \psi)_\Gamma &= (g, \psi)_\Gamma & \psi &\in H_0^1(\Gamma), \\ (\chi, Tu - v)_\Gamma &= (h, \chi)_\Gamma & \chi &\in Q. \end{aligned} \quad (2.3)$$

Letting  $Q = H_{s,0}$ , the well-posedness of (2.3) is guaranteed as the Brezzi conditions are satisfied with  $s = -\frac{1}{2}$ , see [20] for the proof in 2d-1d setting, which immediately generalizes to 3d-2d. Crucial for the well-posedness is the fact that  $T : H_0^1(\Omega) \rightarrow H_{\frac{1}{2},0}(\Gamma)$  is an isomorphism. Consequently, [26] is invoked to yield a block diagonal preconditioner for the discretized problem where individual blocks are conceived as approximations of the corresponding Riesz mappings.

Let now  $V_h \subset H^1(\Omega)$ . Considering (1.1) on the finite dimensional spaces, we obtain a variational problem: Find  $(u_h, v_h, p_h) \in V_h \times W_h \times Q_h$  such that

$$\begin{aligned} (\nabla u_h, \nabla \phi_h)_\Omega + (u_h, \phi_h)_\Omega + (p_h, T_h \phi_h)_\Gamma &= (f, \phi_h)_\Omega & \phi_h &\in V_h, \\ (\nabla v_h, \nabla \psi_h)_\Gamma + (v_h, \psi_h)_\Gamma - (p_h, \psi_h)_\Gamma &= (g, \psi_h)_\Gamma & \psi_h &\in W_h, \\ \langle \chi_h, T_h u_h - v_h \rangle_\Gamma &= (h, \chi_h)_\Gamma & \chi_h &\in Q_h. \end{aligned} \quad (2.4)$$

Here the discrete trace operator  $T_h$  is well-defined as the functions in  $V_h$  are continuous. The continuous problem, on the other hand, is not well defined since  $H^1$  does not permit a bounded trace in  $L^2(\Gamma)$ , see [14]. In turn we cannot directly follow the steps of [20] and employ operator preconditioning [26] to construct an optimal preconditioner. Instead, we shall reason about the properties of the discrete system.

From a linear algebra point of view, the problem (2.4) is a saddle-point system

$$\begin{bmatrix} A & B^\top \\ B & \end{bmatrix} \begin{bmatrix} x \\ y \end{bmatrix} = \begin{bmatrix} b \\ c \end{bmatrix}.$$

Block diagonal preconditioners for such problems can be constructed as an approximate inverse of the matrix  $\text{diag}(\mathbf{K}, \mathbf{L})$ , where  $\mathbf{K}$  should be spectrally equivalent with  $\mathbf{A}$  and  $\mathbf{L}$  should be spectrally equivalent with the Schur complement  $\mathbf{B}\mathbf{A}^{-1}\mathbf{B}^\top$ , see, e.g., [32, 33]. Considering (2.4), the key question is thus whether it is possible (in an efficient and systematic manner) to construct an operator that is spectrally equivalent with the Schur complement. Motivated by the 2d-1d, the operator shall be based on the fractional  $s$ -norm (2.2).

Following [20], the discrete approximation of the  $s$ -norm shall be constructed by mirroring the continuous eigenvalue problem (2.1). More specifically, let  $X_h \subset X$  and matrices  $\mathbf{A}$ ,  $\mathbf{M}$  be the representations of  $A_h$ ,  $M_h$ ; the Galerkin approximations of operators  $A$ ,  $M$  from (2.1). Then there exists an invertible matrix  $\mathbf{U}$  and diagonal, positive-definite matrix  $\Lambda$  satisfying  $\mathbf{A}\mathbf{U} = \mathbf{M}\mathbf{U}\Lambda$ . Moreover, the product  $\mathbf{U}^\top\mathbf{M}\mathbf{U}$  is an identity such that the columns of  $\mathbf{U}$  form an  $\mathbf{A}$  orthogonal and  $\mathbf{M}$  orthonormal basis of  $\mathbb{R}^n$ . In order to define the discrete norm, we let  $\mathbf{H}_s$  be a symmetric, positive-definite matrix

$$\mathbf{H}_s = (\mathbf{M}\mathbf{U})^\top \Lambda^s (\mathbf{M}\mathbf{U}). \quad (2.5)$$

The matrices  $\mathbf{H}_{s,0}$  are defined analogically to (2.5), using the eigenvalue problem for the Laplace operator with homogeneous Dirichlet boundary conditions. For  $u_h \in X_h$  represented in the basis of the space by a coefficient vector  $\mathbf{u}$ , let  $\mathbf{c}$  be the representation of  $\mathbf{u}$  in the basis of eigenvectors, that is,  $\mathbf{u} = \mathbf{U}\mathbf{c}$ . We then set

$$\|u_h\|_{H_s(\Gamma)} = \sqrt{\mathbf{u}^\top \mathbf{H}_s \mathbf{u}} = \sqrt{\mathbf{c}^\top \Lambda^s \mathbf{c}}. \quad (2.6)$$

The generalized eigenvalue problem required for evaluating the discrete  $s$ -norm (2.6) becomes trivial if the approximation space  $V_n$  is such that  $V_n = \text{span}\{\phi_i\}_{i=1}^n$ , i.e. the basis is formed by the eigenvectors of the continuous problem (2.1). Such a discretization is practically limited to Cartesian domains, however, it will prove useful in studying the trace operator when the codimension of  $\Gamma$  in  $\Omega$  is two. The technique is introduced in Example 2.1.

**EXAMPLE 2.1** (Spectral method for 2d-1d coupled problem). *Let  $\Omega = [0, 1]^2$ ,  $\Gamma = \{(t, \frac{1}{2}); t \in [0, 1]\}$  and consider the task of finding  $u \in H^1(\Omega)$  which minimizes  $v \mapsto (\nabla v, \nabla v)_\Omega - 2(f, v)_\Omega$  subject to  $Tu = g$  and  $u = 0$  on the boundary (in the sense of traces). Introducing  $V = H_0^1(\Omega)$ ,  $Q = H_{-\frac{1}{2},0}(\Gamma)$  the problem is formulated as a saddle point system for  $u \in V$ ,  $p \in Q$  satisfying*

$$\begin{aligned} (\nabla u, \nabla v)_\Omega + \langle p, Tv \rangle_{Q',Q} &= (f, v)_\Omega & v \in V, \\ \langle q, Tu \rangle_{Q',Q} &= \langle q, g \rangle_{Q',Q} & q \in Q. \end{aligned} \quad (2.7)$$

*Well-posedness of (2.7) is readily established by verifying the Brezzi conditions [9]. In particular, the inf-sup condition can be shown to hold, see, e.g., Appendix A. By operator preconditioning [26] the canonical preconditioner for (2.7) is the Riesz map with respect to the inner product inducing the norm of  $V \times Q$ .*

*The Galerkin approximation of (2.7) is defined with spaces  $Q_m$ ,  $V_n$  such that  $Q_m = \text{span}\{\phi_k(t)\}_{k=1}^m$  and  $V_n = \text{span}\{\phi_i(x)\phi_j(y)\}_{i,j=1}^n$ . Recall that functions  $\phi_k(t) = \sqrt{2}\sin k\pi t$  are the eigenfunctions of (2.1) satisfying  $-\Delta\phi_k = (k\pi)^2\phi_k$  on  $\Gamma$ . For greater readability, let us introduce  $N = n^2$ . In the basis of eigenfunctions, the discrete trace operator is represented by a trace matrix  $\mathbf{T} \in \mathbb{R}^{m \times N}$  with entries*

$$\mathbf{T}_{k,(i,j)} = \begin{cases} 0 & j \text{ even} \\ (-1)^{j+1}\sqrt{2}\delta_{ik} & j \text{ odd} \end{cases}.$$

Here  $(i, j)$  is a column index  $n(i-1) + j$ . With matrix  $\mathbf{A} \in \mathbb{R}^{N \times N}$  and vectors  $\mathbf{f} \in \mathbb{R}^N$ ,  $\mathbf{g} \in \mathbb{R}^m$  defined in a natural way, the preconditioned linear system from (2.7) is

$$\begin{bmatrix} \mathbf{A} & \\ & \mathbf{H}_{-\frac{1}{2},0} \end{bmatrix}^{-1} \begin{bmatrix} \mathbf{A} & \mathbf{T}^\top \\ \mathbf{T} & \end{bmatrix} \begin{bmatrix} \mathbf{u} \\ \mathbf{p} \end{bmatrix} = \begin{bmatrix} \mathbf{A} & \\ & \mathbf{H}_{-\frac{1}{2},0} \end{bmatrix}^{-1} \begin{bmatrix} \mathbf{f} \\ \mathbf{g} \end{bmatrix}, \quad (2.8)$$

where the first matrix is the discretization of the canonical preconditioner. We note that matrices  $\mathbf{H}_{s,0}$  are diagonal. Consequently  $\mathbf{H}_{s,0}^{-1} = \mathbf{H}_{-s,0}$ .

For stability of the solution obtained by solving (2.8), it is required that the discrete inf-sup condition holds. Note that for  $m > n$  the trace matrix does not have a full row rank and thus  $m \leq n$  is necessary. We shall set  $m = n$  and show that for this choice the inf-sup condition is satisfied.

By, e.g., [24] or [7], the constant of the discrete inf-sup condition is the smallest eigenvalue of the generalized eigenvalue problem for the negative Schur complement of the system matrix, i.e.,

$$\mathbf{T}\mathbf{A}^{-1}\mathbf{T}^\top \mathbf{e} = \lambda \mathbf{H}_{-\frac{1}{2},0} \mathbf{e},$$

where  $(\lambda \in \mathbb{R}, \mathbf{e} \in \mathbb{R}^m)$  is the sought eigenpair. The simple structure of the involved matrices allows us to compute all the eigenvalues of the problem analytically. In fact,

$$(\mathbf{H}_{\frac{1}{2},0} \mathbf{T}\mathbf{A}^{-1}\mathbf{T}^\top)_{ij} = S_j \delta_{ij} \text{ where } S_j = \frac{2}{\pi} \sum_{l \text{ odd}}^n \frac{j}{j^2 + l^2}.$$

Then  $S_j \geq S_n$  and the lower bound can be evaluated. Using Mathematica [36], we have obtained  $\lim_{n \rightarrow \infty} S_n = \frac{1}{8}$  as the discrete inf-sup constant. For the largest eigenvalue, the following estimate can be established

$$S_j \leq \frac{2}{\pi} \sum_{l \text{ odd}}^{\infty} \frac{j}{j^2 + l^2} = \frac{1}{4} \tanh \frac{j\pi}{2} \leq \frac{1}{4}$$

and in turn the theoretical spectral condition number for the preconditioned Schur complement is  $\kappa = 2$ . We remark that the remaining Brezzi constants are both equal to one and the condition number of (2.8) can be determined from spectral bounds presented in [32].

The theoretical findings about the condition number of the preconditioned Schur complement are confirmed by numerical experiments, with results shown in Figure 2.1 and Table 2.1. The figure shows that there is a range of exponents  $s \in [-0.52, -0.5]$  for which the condition numbers are stable. Interestingly, in this range  $s = -0.5$  gives the largest condition number while for  $s = -0.52$  a slightly smaller value is observed, cf. Table 2.1.

**3. Norms for the discrete 3d-1d trace.** In Example 2.1 a priori knowledge of the trace space lead to an optimal preconditioner for the model problem (2.7). In particular, the norm of the trace space was used to construct a spectrally equivalent operator to the Schur complement of (2.8). For  $\Omega \subset \mathbb{R}^3$  and  $\Gamma$  a one dimensional curve, the trace space is not a priori known and we shall therefore attempt to characterize it numerically. To this end, we shall at first use the spectral discretization and search for the  $s$ -norm (2.6) for which the condition number of the preconditioned Schur complement is bounded in the discretization parameter. We note that the condition is motivated by the fact that convergence of the preconditioned conjugate gradient

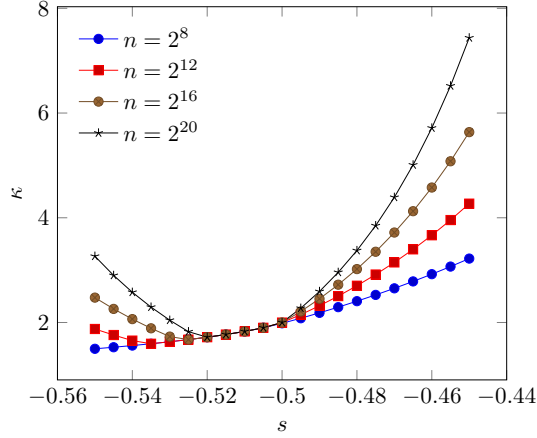


Fig. 2.1: Spectral condition numbers of the generalized eigenvalue problem for matrices  $\mathbf{T}\mathbf{A}^{-1}\mathbf{T}^\top$  and  $\mathbf{H}_{s,0}$ , (cf. (2.8)), and different values of the discretization parameter  $n$ . The exponent  $s = -\frac{1}{2}$  yields condition number 2, independent of  $n$ . Only the exponents  $s \in [-0.52, 0.5]$  yield stable condition numbers.

Table 2.1: Spectral condition numbers  $\kappa$  of the preconditioned Schur complement of (2.8) with two preconditioners  $\mathbf{H}_{-0.5,0}$  and  $\mathbf{H}_{-0.52,0}$ . In agreement with analysis,  $s = -0.5$  yields bounded  $\kappa$ . The value  $s = -0.52$ , determined from observations, cf. Figure 2.1, yields a smaller condition number.

$\log_2 n$	8	10	12	14	16	18	20
$s = -0.5$	1.9848	1.9959	1.9987	1.9997	1.9999	2.0000	2.0000
$s = -0.52$	1.7189	1.7190	1.7190	1.7190	1.7190	1.7190	1.7190

method is estimated in terms of the condition number, see, e.g., [35]. For suitable  $s$  the linear system with the Schur complement could thus be solved efficiently. We also note that the condition is weaker than spectral equivalence. In fact, if such  $s$  exists, the matrix  $\mathbf{H}_{s,0}$  is spectrally equivalent with the Schur complement if and only if one of the extremal eigenvalues is bounded by a constant.

**3.1. Trace operator with spectral discretization.** Let  $\Omega = [0, 1]^3$ ,  $Q_m = \text{span}\{\phi_j(t)\}_{j=1}^m$  and  $V_n = \text{span}\{\phi_i(x)\phi_k(y)\phi_l(z)\}_{i,k,l=1}^n$ , cf. Example 2.1. We consider the problem of minimizing  $v \mapsto (\nabla v, \nabla v)_\Omega - 2(f, v)_\Omega$ ,  $v \in V_n$ , subject to  $v = 0$  on the boundary and the constraint  $Tv = g$  on  $\Gamma$ , where the trace operator restricts  $v$  either to  $\Gamma_1 = \{(t, \frac{1}{2}, \frac{1}{2}); t \in [0, 1]\}$  or  $\Gamma_2 = \{(t, t, t); t \in [0, 1]\}$  respectively. The weak formulation of the problem reads

$$\begin{aligned} (\nabla u, \nabla v)_\Omega + (p, Tv)_\Gamma &= (f, v)_\Omega & v \in V_n, \\ (q, Tu)_\Gamma &= (q, g)_\Gamma & q \in Q_m \end{aligned} \quad (3.1)$$

and is equivalent with a linear system

$$\begin{bmatrix} \mathbf{A} & \mathbf{T}^\top \\ \mathbf{T} & \end{bmatrix} \begin{bmatrix} \mathbf{u} \\ \mathbf{p} \end{bmatrix} = \begin{bmatrix} \mathbf{f} \\ \mathbf{g} \end{bmatrix}. \quad (3.2)$$



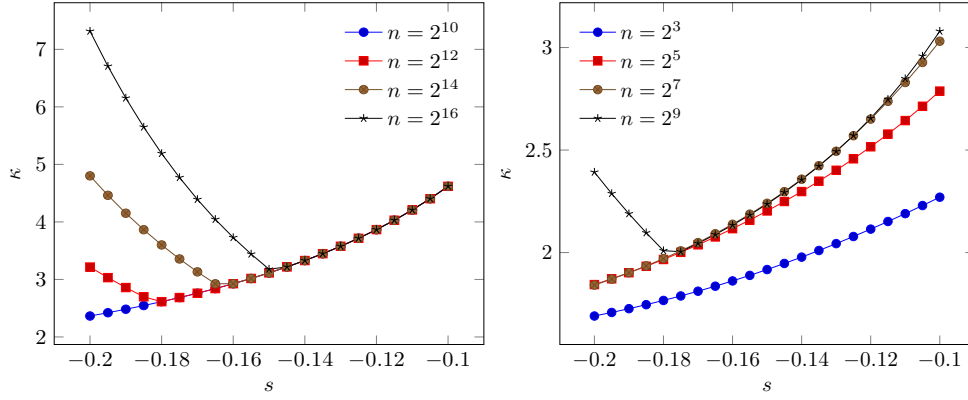


Fig. 3.1: Spectral condition numbers computed from the generalized eigenvalue problem for Schur complement of (3.2) and matrices  $H_{s,0}$ , see (2.6). (Left) The constraint is considered on  $\Gamma = \{(t, \frac{1}{2}, \frac{1}{2}); t \in [0, 1]\}$ . (Right)  $\Gamma = \{(t, t, t); t \in [0, 1]\}$  is considered. With both configurations, values  $s$  close to  $-0.14$  yield bounded  $\kappa$ .

In (3.2) the trace matrix  $T \in \mathbb{R}^{m \times N}$  for curve  $\Gamma_1$  is sparse with entries

$$T_{j,(i,k,l)} = \begin{cases} 0 & k \text{ or } l \text{ even} \\ (-1)^{k+1}(-1)^{l+1}2\delta_{ij} & \text{otherwise} \end{cases}.$$

Here  $N = n^3$  was introduced for readability. Note that for  $m > n$  the matrix does not have a full row rank and the system is singular. We therefore set  $m = n$ . For  $\Gamma_2$  the trace matrix is sparse with a more involved sparsity pattern and at most four nonzero entries per row

$$T_{j,(i,k,l)} = 4\sqrt{3} \int_0^1 \sin j\pi t \sin i\pi t \sin k\pi t \sin l\pi t dt.$$

Finally, we consider the generalized eigenvalue problem for the Schur complement of (3.2) and matrices  $H_{s,0}$  where such exponents are of interest, for which the spectral condition number  $\kappa = \lambda_{\max}/\lambda_{\min}$  is bounded in the discretization parameter. Note that with  $\Gamma_1$  the Schur complement is a diagonal matrix  $S_j \delta_{ij}$ ,

$$S_j = \frac{4}{\pi^2} \sum_{l,m \text{ odd}}^n \frac{1}{j^2 + l^2 + m^2}. \quad (3.3)$$

For  $\Gamma_2$  the matrix is dense and shall be computed from assembled terms. As such a smaller  $n$  is explored in this configuration.

The results of the numerical experiments with  $s \in [-0.2, -0.1]$  are summarized in Figure 3.1. We observe that values  $s \in [-0.145, -0.1]$  yield bounded condition numbers for  $\Gamma_1$ . The condition numbers are not quite converged for the other configuration, however, it is possible to identify unstable exponents  $s < -0.18$ . Moreover, the values close to  $s = -0.14$  appear to be stable also in this configuration. This fact is easier to appreciate in Table 3.1, which shows  $\lambda_{\min}$ ,  $\lambda_{\max}$  and  $\kappa$  as functions of the discretization parameter for  $s = -0.14$ . With  $\Gamma_1$  the condition number is evidently



Table 3.1: Smallest and largest eigenvalues  $\lambda_{\min}$ ,  $\lambda_{\max}$  and the spectral condition numbers  $\kappa$  of the preconditioned Schur complement of (3.2). (Top) The preconditioner is  $H_{-0.14,0}$ . While the eigenvalues are unbounded the condition number is bounded in  $n$ . (Bottom) Matrix  $H_{0,0}$  (identity matrix) is used as the preconditioner. In agreement with the analysis in Remark 3.1, constant  $\lambda_{\min}$  and  $\lambda_{\max}$  with a logarithmic growth are observed.

$\Gamma = \{(t, \frac{1}{2}, \frac{1}{2}); t \in [0, 1]\}$				$\Gamma = \{(t, t, t); t \in [0, 1]\}$			
$\log_2 n$	$\lambda_{\min}$	$\lambda_{\max}$	$\kappa$	$\log_2 n$	$\lambda_{\min}$	$\lambda_{\max}$	$\kappa$
10	0.6218	2.0696	3.3285	6	0.8476	1.9916	2.3496
12	0.9167	3.0511	3.3285	7	1.0298	2.4283	2.3581
14	1.3514	4.4982	3.3285	8	1.2513	2.9491	2.3569
16	1.9923	6.6315	3.3285	9	1.5201	3.5804	2.3553
11	0.0648	1.2167	18.7767	6	0.1939	1.2180	6.2807
12	0.0648	1.3270	20.4792	7	0.1938	1.4080	7.2655
13	0.0648	1.4373	22.1818	8	0.1938	1.5985	8.2487
14	0.0648	1.5476	23.8843	9	0.1938	1.7893	9.2312

constant, while for  $\Gamma_2$  the number appears to be bounded. Note that with both configurations the smallest and largest eigenvalues are not bounded and thus  $H_{-0.14,0}$  is not spectrally equivalent with the Schur complement with the bounds independent of  $n$ . However, any of  $\lambda_{\min}(n)$ ,  $\lambda_{\max}(n)$  (or their linear combinations) define a mesh-dependent scale  $\tau(n)H_{-0.14,0}$  that yields spectral equivalence. Such scale, however, is not easily computable in general.

In the numerical experiment the range of exponents was limited to  $s \in [-0.2, -0.1]$  and the upper bound yielded condition numbers independent of the discretization parameter, cf. Figure 3.1. The observation raises a question about the suitability of  $s = 0$ , i.e. considering the multiplier space  $Q_m$  with the  $L^2$  norm. It is shown in Remark 3.1 that the choice leads to a condition number with logarithmic growth.

REMARK 3.1. We consider (3.2) with  $\Gamma_1$ . Since  $H_{0,0}$  is (due to the employed discretization) an identity, the values  $S_j$  in (3.3) are the eigenvalues of the preconditioned Schur complement, where  $H_{0,0}$  is the preconditioner. We have  $S_j \geq S_n$  and observe that the lower bound sums  $\mathcal{O}(n^2)$  terms that are at most  $n^{-2}$  in magnitude. Thus  $S_n$  is bounded from below by a constant. On the other hand the upper bound  $S_j \leq S_1$  grows as  $\log n$ .

Note that for the 2d-1d trace and  $s = 0$  we have, cf. Example 2.1,

$$\frac{2}{\pi} \sum_{l \text{ odd}}^n \frac{1}{n^2 + l^2} \leq S_j = \frac{2}{\pi} \sum_{l \text{ odd}}^n \frac{1}{j^2 + l^2} \leq \frac{2}{\pi} \sum_{l \text{ odd}}^n \frac{1}{1 + l^2} \leq C,$$

while the lower bound as a sum of  $\mathcal{O}(n)$  terms with  $n^{-2}$  magnitude decays as  $n^{-1}$ . Thus  $s = 0$  leads to a linearly growing condition number.

The estimates for  $\Omega \subset \mathbb{R}^3$  are confirmed by numerical experiment summarized in Table 3.1. In particular, the constant lower bound and the upper bound growing as  $\log n$ , are visible for both configurations.

Experiments with the spectral discretization suggest that there exists an exponent  $s$ , independent of  $\Gamma$ , such that the discrete trace operator  $T_h$  defined over  $V_h$  can be controlled by the  $s$ -norm (2.6). However, the space  $V_h$  considered thus far consisted of infinitely smooth functions. We proceed to show that a similar conjecture holds if the discrete spaces are obtained by FEM. In particular, the space  $V_h$  shall be constructed

using the  $H^1$  conforming continuous linear Lagrange elements.

**3.2. Trace operator with FEM discretization.** Let  $V_h \subset H^1(\Omega)$ . Further, let  $\{\psi_k\}_{k=1}^m$  and  $\{L_j\}_{j=1}^m$  be, respectively, the basis and degrees of freedom/dual basis nodal with respect to  $\{\psi_k\}_{k=1}^m$  of the finite element space  $Q_h$  over  $\Gamma$ . The trace mapping  $T_h : V_h \rightarrow Q_h$  shall be defined by interpolation so that  $p_h = T_h u_h$  is represented in the basis by vector  $\mathbf{p} \in \mathbb{R}^m$ ,

$$\mathbf{p}_j = \langle L_j, u_h|_\Gamma \rangle. \quad (3.4)$$

Equivalently we have  $\mathbf{p} = \mathbf{T}\mathbf{u}$  where  $\mathbf{u} \in \mathbb{R}^n$  and the matrix representing the trace operator has entries

$$\mathbf{T}_{i,j} = \langle L_i, \phi_j|_\Gamma \rangle,$$

where  $\{\phi_j\}_{j=1}^n$  are the basis functions of  $V_h$ .

LEMMA 3.1 (Discrete trace operator by projection). *Let  $u_h \in V_h$  be given and  $\tilde{p}_h \in Q_h$  be the  $L^2$  projection*

$$(\tilde{p}_h, q)_\Gamma = (u_h|_\Gamma, q)_\Gamma, \quad q \in Q_h.$$

*Further let  $p_h \in Q_h$  be defined via (3.4). Then  $V_h|_\Gamma \subseteq Q_h$  is necessary and sufficient for  $p_h = \tilde{p}_h$ .*

*Proof.* To verify the assertion let  $q_k \in Q_h$  be the Riesz representation of  $L_k$ , i.e.  $(q_k, v)_\Gamma = \langle L_k, v \rangle$ ,  $v \in Q_h$ , and  $u_h \in V_h$  arbitrary. Then by definition  $(p_h, q_k)_\Gamma = \langle L_i, u_h|_\Gamma \rangle (\psi_i, q_k)_\Gamma$  and

$$\langle L_i, u_h|_\Gamma \rangle (\psi_i, q_k)_\Gamma = (q_i, u_h|_\Gamma)_\Gamma \langle L_k, \psi_i \rangle = (q_k, u_h|_\Gamma)_\Gamma = (q_k, \tilde{p}_h)_\Gamma$$

by the property of the Riesz basis  $\{q_k\}_{k=1}^m$ , nodality of the basis  $\{\psi_i\}_{i=1}^m$  and definition of  $\tilde{p}_h$ . It follows that  $(p_h - \tilde{p}_h, q_k)_\Gamma = 0$ . Note that  $u_h|_\Gamma \in Q_h$  was required to apply the Riesz theorem.  $\square$

DEFINITION 3.2 ( $\Gamma$ -matching spaces). *Let  $\Gamma$  be a manifold in  $\Omega$  and  $Q_h, V_h$  the finite element spaces over the respected domains. The spaces are called  $\Gamma$ -matching if (i)  $V_h$  and  $Q_h$  are constructed from the same elements and (ii) meshes of  $\Omega$  and  $\Gamma$  are matched.*

REMARK 3.2 (Equivalence of interpolation and projection trace). *The condition from Lemma 3.1 is satisfied with  $V_h|_\Gamma = Q_h$  if  $V_h$  and  $Q_h$  are  $\Gamma$ -matching. Finally, note that the interpolation trace is in general cheaper to construct than the trace due to projection. We shall employ (3.4) throughout the rest of the paper.*

Let now  $V_h, Q_h$  be a pair of  $\Gamma$ -matching spaces constructed from continuous linear Lagrange elements. Further, the discretization of the geometry shall be such that the mesh of  $\Omega$  is *finer* at/near  $\Gamma$  than in the rest of the domain, cf. Table B.1 in Appendix B and Figure 4.1. This way the dimensionality of  $Q_h$  is increased. Finally, we consider the Schur complement<sup>1</sup> of (3.1) preconditioned by different matrices  $\mathbf{H}_{s,0}$ . Recall that previously global trigonometric polynomial basis functions were used with (3.1) and  $-0.2 < s \leq -0.1$  yielded condition numbers bounded in the discretization parameter. Figure 3.2 and Table 3.2 show that the same conclusions hold also if the finite element discretization is employed.

<sup>1</sup> The Schur complement is computed from its definition, where the components  $\mathbf{T}$ ,  $\mathbf{A}$  are assembled using FEniCS [23, 2] and PETSc [8] libraries. The Laplacian matrix is then inverted by conjugate gradient method with algebraic multigrid (AMG) preconditioner from Hypre library [15]. Relative tolerance  $10^{-15}$  was set as a convergence criterion.

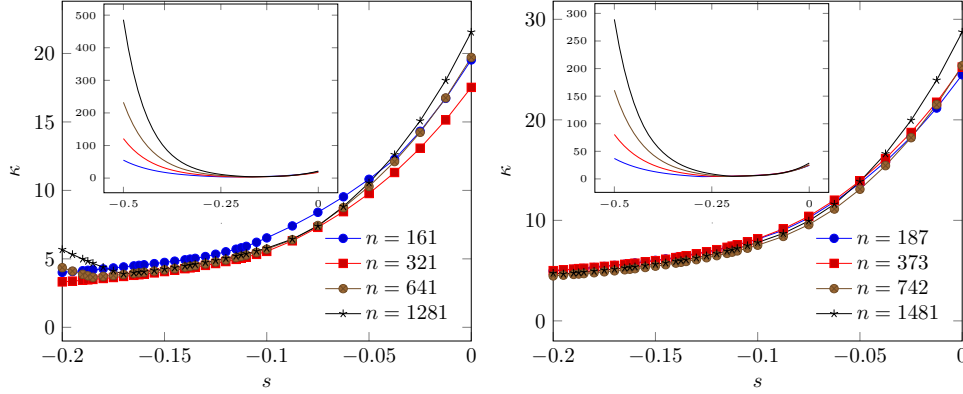


Fig. 3.2: Condition numbers of the Schur complement of (3.1) with finite element discretization,  $n = \dim Q_h$ , and different preconditioners  $H_{s,0}$ . (Left) the curve is  $\Gamma_1$ . (Right) the curve is  $\Gamma_2$ . The zoomed out plot shows that  $s < -0.25$  yields unbounded  $\kappa$ . For both configurations exponents from the interval around  $s = -0.1$  yield bounded condition numbers.

Table 3.2: Condition numbers of  $H_{s,0}$  preconditioned Schur complement of (3.1) for selected values of  $s$ . The finite element discretization is considered on a sequence of uniformly refined meshes, see Table B.1. For each discretization the mesh is finer near  $\Gamma$  than in the rest of the domain. Exponent  $s = -0.14$  observed in the spectral discretization, cf. Table 3.1, yields bounded  $\kappa$  also with discretization by FEM. Note that similar to the spectral discretization there is a slight growth of  $\kappa$  for  $s = 0$ .

$L \setminus s$	$\Gamma = \{(t, \frac{1}{2}, \frac{1}{2}); t \in [0, 1]\}$					$\Gamma = \{(t, t, t); t \in [0, 1]\}$				
	-0.16	-0.14	-0.12	-0.1	0	-0.16	-0.14	-0.12	-0.1	0
1	4.568	4.932	5.517	6.531	19.530	5.760	6.316	7.064	8.129	24.484
2	3.883	4.282	4.804	5.545	17.525	5.743	6.300	7.085	8.175	25.253
3	4.023	4.400	4.927	5.710	19.713	5.192	5.744	6.488	7.525	25.386
4	4.062	4.477	5.045	5.781	21.561	5.381	5.926	6.698	7.798	28.731

Figure 3.2 explores the condition numbers for  $s \in [-0.5, 0]$ . It is evident, cf. the zoom-out plot, that for  $s < -0.25$ ,  $H_{s,0}$  is not a good preconditioner for the Schur complement. For both configurations there are exponents in  $(-0.2, 0)$  that lead to bounded condition numbers. For several values of  $s$  in this interval, the condition numbers observed on a sequence of uniformly refined meshes are reported in Table 3.2. Therein  $s \leq -0.1$  can be observed to lead to bounded  $\kappa$ . Exponent  $s = 0$ , i.e. the  $L^2$  norm, leads to a slight growth in  $\kappa$  with both  $\Gamma_1$  and  $\Gamma_2$ .

We note that in both configurations the behaviour of the eigenvalues is similar to the spectral case. In particular,  $\lambda_{\max}$  and  $\lambda_{\min}$  grow for  $s \leq -0.1$ , whereas for  $s = 0$  only  $\lambda_{\max}$  grows while  $\lambda_{\min}$  is bounded by a constant, see Table 3.3. Since the extremal eigenvalues are in general not bounded by a constant,  $H_{s,0}$  is not a discretization of an operator spectrally equivalent to the Schur complement with constants independent of the discretization parameter. However, the relation observed in the experiments

$$0 < \lambda_{\min}(h) \leq \frac{\mathbf{x}^\top \mathbf{T} \mathbf{A}^{-1} \mathbf{T}^\top \mathbf{x}}{\mathbf{x}^\top \mathbf{H}_{s,0} \mathbf{x}} \leq \lambda_{\max}(h) \quad \mathbf{x} \in \mathbb{R}^m \quad (3.5)$$

Table 3.3: Smallest and largest eigenvalues of the  $H_{s,0}$  preconditioned Schur complement considered in Table 3.2. Similar to spectral discretization both the extremal eigenvalues grow for  $s = -0.14$  while the lower bound is constant and the upper one grows for  $s = 0$ .

L	$\Gamma = \{(t, \frac{1}{2}, \frac{1}{2}); t \in [0, 1]\}$		$\Gamma = \{(t, t, t); t \in [0, 1]\}$	
	$s = -0.14$	$s = 0$	$s = -0.14$	$s = 0$
1	(0.290, 1.433)	(0.051, 1.000)	(0.207, 1.310)	(0.041, 1.000)
2	(0.420, 1.799)	(0.059, 1.040)	(0.256, 1.610)	(0.041, 1.026)
3	(0.502, 2.208)	(0.059, 1.161)	(0.342, 1.965)	(0.045, 1.145)
4	(0.603, 2.701)	(0.059, 1.276)	(0.401, 2.379)	(0.044, 1.265)

suggests existence of a mesh dependent scale in which spectral equivalence can be achieved. In particular, rescaling the  $s$ -norm matrix as  $\lambda_{\min}(h)H_{s,0}$  leads to constant bounds, cf. observed constant spectral condition number. We remark that  $\lambda_{\min}$  is bounded away from zero for all  $h$ , in fact the eigenvalue increases with  $h^{-1}$ , and in this sense the discrete inf-sup constant never approaches zero.

Based on the mesh-dependent  $s$ -norm a block-diagonal preconditioner  $\text{diag}(A, \lambda_{\min}(h)H_{s,0})^{-1}$  could be analysed and shown to be optimal using the results of [32, 33] (see also the review paper [29]). However, obtaining the scale is computationally expensive. We shall therefore proceed with (2.6) only. In particular, the exponents  $s$  identified previously shall be used to construct preconditioners for several 3d-1d constrained problems. We note that the bounds (3.5) enter estimates for convergence of iterative solvers, see, e.g., [33], and since the bounds here are not constant, the proposed preconditioners are theoretically suboptimal. Nevertheless, the number of iterations in the studied examples will be bounded. We remark that the smallest and largest eigenvalues are never far from unity in our examples.

**4. Trace coupled problems.** The previous experiments revealed a range of exponents  $s$  for which matrices  $H_s$  behaved similarly to the Schur complement, in terms of stability of the condition number, of the related generalized eigenvalue problem. To simplify the discussion, we shall in the following employ  $s = -0.14$ . The exponent shall be used to construct preconditioners for two model 3d-1d coupled problems.

**4.1. Babuška's problem.** Let  $V_h, Q_h$  be a pair of  $\Gamma$ -matching spaces constructed by continuous linear Lagrange elements and consider the problem: Find  $u \in V_h \subset H^1(\Omega), p \in Q_h$  such that

$$\begin{aligned} (\nabla u, \nabla v)_\Omega + (u, v)_\Omega + (p, Tv)_\Gamma &= (f, v)_\Omega & v \in V_h, \\ (q, Tu)_\Gamma &= (q, g)_\Gamma & q \in Q_h. \end{aligned} \quad (4.1)$$

The system (4.1) is a Lagrange multiplier formulation of the minimization problem for  $v \mapsto \|v\|_{H^1(\Omega)}^2 - 2(f, v)_\Omega$ , and the constraint  $Tv - g = 0$  on  $\Gamma$ . We note that the problem is considered with homogeneous Neumann boundary conditions. A similar problem with  $\Omega \subset \mathbb{R}^2$  and  $\Gamma \subset \partial\Omega$  was first studied in [6] to introduce Lagrange multipliers as means of prescribing boundary data.

Similar to the Schur complement study in Section 3.2, the problem shall be considered with two different curves  $\Gamma$ . Moreover, for each configuration we consider three different sequences of uniformly refined meshes, to investigate numerically whether the construction of the preconditioner relies on a quasi-uniform mesh, or if shape-regular elements are sufficient. In a *uniform* discretization the characteristic mesh

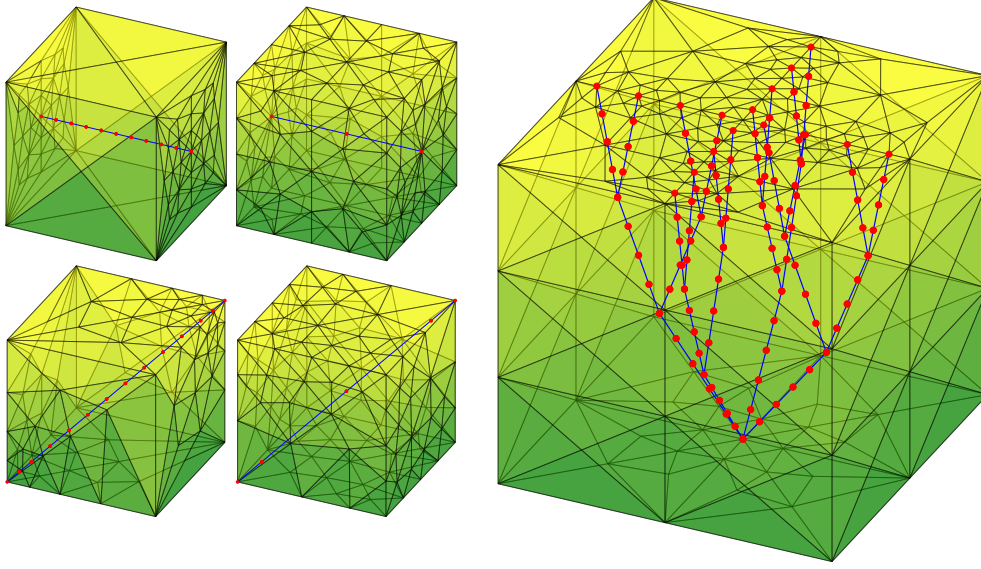


Fig. 4.1: Domains used in experiments with matching discretization. The one dimensional curve  $\Gamma$  is drawn in blue with element boundaries signified by red dots. (Left) The curve is, respectively, a horizontal or diagonal segment. The triangulation of  $\Omega$  is either refined or coarsened at  $\Gamma$ . (Right) The curve contains branches and bifurcations, thus capturing some of the features of complex vascular systems.

size of  $\Omega$  and  $\Gamma$  are identical and the tessellation of  $\Omega$  is structured. In *finer* and *coarser* discretizations the mesh is unstructured and is either finer or coarser near  $\Gamma$  than in the rest of the domain. The example meshes are pictured in Figure 4.1. Information about the parameters of the discretizations and sizes of the corresponding finite element spaces are then summarized in Table B.1.

Since (4.1) is considered with Neumann boundary conditions, the block diagonal preconditioner for the system shall have the multiplier block based on  $H_s$  (not  $H_{s,0}$ ). We propose the following preconditioned linear system

$$\begin{bmatrix} A + M & \\ & H_{-0.14} \end{bmatrix}^{-1} \begin{bmatrix} A + M & (M_\Gamma T)^\top \\ (M_\Gamma T) & \end{bmatrix} \begin{bmatrix} u \\ p \end{bmatrix} = \begin{bmatrix} A + M & \\ & H_{-0.14} \end{bmatrix}^{-1} \begin{bmatrix} f \\ g \end{bmatrix}, \quad (4.2)$$

where  $M$  and  $M_\Gamma$  are, respectively, the mass matrices of  $V_h$  and  $Q_h$ . We remark that the proposed preconditioner is not theoretically optimal because of the estimate (3.5).

In our implementation the leading block of the preconditioner is inverted by algebraic multigrid from the Hypre<sup>2</sup> library [15]. The system is then solved iteratively with the minimal residual method (MINRES) implemented in cbc.block [25] and requiring a preconditioned residual norm smaller than  $10^{-12}$  for convergence. The initial vectors were random.

The recorded iterations counts are reported in Table 4.1. It can be seen that the proposed preconditioner results in a bounded number of iterations for all the considered geometrical configurations and their discretizations. In the table we also

---

<sup>2</sup>We have used default values of all the parameters.

Table 4.1: Iteration counts for preconditioned Babuška's problem (4.1) with preconditioners based on (2.5) and  $s = -0.14$  or  $s = 0$  (discrete  $L^2$  norm). Two geometric configurations and their different discretizations ( $L$  denotes the refinement level) are considered cf. Figure 4.1 and Table B.1. Both preconditioners yield bounded number of iterations. The  $L^2$  norm leads to a less efficient preconditioner.

L	$\Gamma = \{(t, \frac{1}{2}, \frac{1}{2}); t \in [0, 1]\}$			$\Gamma = \{(t, t, t); t \in [0, 1]\}$		
	uniform	finer	coarser	uniform	finer	coarser
2	(28, 59)	(53, 81)	(44, 46)	(29, 57)	(73, 107)	(62, 71)
3	(27, 68)	(52, 82)	(49, 58)	(27, 59)	(69, 103)	(64, 81)
4	(25, 70)	(52, 83)	(47, 62)	(25, 61)	(69, 105)	(67, 88)
5	(23, 70)	(53, 83)	(51, 71)	(25, 62)	(70, 105)	(67, 91)

report iteration counts for the preconditioner that employs  $H_0 = M_\Gamma$  for the multiplier block. Recall that with  $s = 0$  and spectral discretization, the spectral condition number of the preconditioned Schur complement showed a logarithmic growth, cf. Table 3.1. Using FEM, the growth was less evident (see Table 3.2), however, the condition number was significantly larger than for  $s = -0.14$ . The iteration counts agree with this observation; the  $L^2$  norm leads to at least 20 more iterations. We remark that the norms in which the convergence criterion is measured differ between the two cases.

**4.2. Model multiphysics problem.** Building upon the Babuška problem we next consider a model multiphysics problem (1.1). A similar problem with  $\Omega \subset \mathbb{R}^2$  and  $\Gamma$  a manifold of codimension one was previously studied by the authors in [20]. Therein it was found that the problem is well posed with the Lagrange multiplier in the intersection space  $H^{-\frac{1}{2}}(\Gamma) \cap H^{-1}(\Gamma)$ . The structure of the space was mirrored by the preconditioner, which used  $(H_{-0.5} + H_{-1})^{-1}$  in the corresponding block.

We note that the exponent  $-\frac{1}{2}$  was dictated by the properties of the continuous trace operator. In the 3d-1d case, which is of interest here, we shall instead base the exponent/preconditioner on the previous numerical experiments. More specifically, the linear system obtained by considering (2.4) on finite dimensional finite element subspaces

$$\begin{bmatrix} A_\Omega + M_\Omega & & (M_\Gamma T)^\top \\ & A_\Gamma + M_\Gamma & M_\Gamma \\ (M_\Gamma T) & & M_\Gamma \end{bmatrix} \begin{bmatrix} u \\ w \\ p \end{bmatrix} = \begin{bmatrix} f \\ g \\ h \end{bmatrix} \quad (4.3)$$

shall be considered with the preconditioner

$$\begin{bmatrix} A_\Omega + M_\Omega & & \\ & A_\Gamma + M_\Gamma & \\ & & H_{-0.14} + H_{-1} \end{bmatrix}^{-1}. \quad (4.4)$$

Note that in (4.4) the structure of the trailing block mimics the related 2d-1d problem. We remark that in the implementation, the remaining two blocks are inverted by AMG. Moreover the discrete spaces are such that  $W_h = Q_h$  and  $V_h, Q_h$  are  $\Gamma$ -matching. As in the previous example, continuous linear Lagrange elements are used. To demonstrate the performance of the preconditioner, (2.4) is considered on the same geometrical configurations and their discretizations as (4.1). The preconditioned system is then solved by MINRES, starting from a random initial vector and terminating

Table 4.2: Iteration counts for the model problem (4.3) with preconditioner (4.4). Spatial configurations and discretizations from Table 4.1 are considered. In all the cases the number of iterations is bounded.

L	$\Gamma = \{(t, \frac{1}{2}, \frac{1}{2}); t \in [0, 1]\}$			$\Gamma = \{(t, t, t); t \in [0, 1]\}$		
	uniform	finer	coarser	uniform	finer	coarser
2	51	45	42	44	62	62
3	49	45	48	43	59	62
4	47	43	47	43	59	64
5	46	43	49	42	59	66

if the preconditioned residuum is less than  $10^{-12}$  in magnitude. As can be seen in Table 4.2, the preconditioner yields bounded iteration counts. Interestingly, the convergence is faster on the *finer* discretization than on the *coarser* one. We note that the systems on the latter discretization are in general of smaller size and have more than a factor 10 fewer degrees of freedom in  $Q_h$ .

In the examples presented thus far,  $\Gamma$  was always a straight segment. To show that the preconditioner (4.4) (or the general idea of  $H_s$  based preconditioners for  $3d-1d$  problems) is not limited to such simple curves, we shall in the final example consider (2.4) with  $\Gamma$  having a more complicated structure. The considered domain, pictured in the right pane of Figure 4.1, is inspired by biomechanical applications and is intended to mimic some of the features of the vasculature. In particular, the domain consists of numerous branches and contains multiple bifurcations.

Repeating the setup of the previous experiment, Table 4.3 reports the iteration counts for the (4.4) preconditioned linear system (4.3), obtained by considering (2.4) on the complex  $\Gamma$ . The number of iterations is clearly bounded. In fact, the number decreases with refinement.

The good performance of the proposed preconditioner in all the considered examples brings in the question of practicability of its construction. Here, the question shall be addressed by considering the setup costs of the preconditioner for the domain with complex  $\Gamma$ . The choice is motivated by the fact that (i) the domain is potentially relevant for practical applications and (ii) the large (relative to  $\dim V_h$ ) number of degrees of freedom of  $Q_h$  puts the emphasis on the construction of (2.5). We note that the costs are expected to be determined by the multigrid setup and the solution time of the generalized eigenvalue problem (2.5). As in [20] the eigenvalue problem is solved by the DSYGVD routine from LAPACK [3].

The timings obtained on a Linux machine with a single Intel Xeon E5-2680 CPU with 2.5GHz and 32GB of RAM are reported in Table 4.3. The observed costs of the eigenvalue solve are 3-4 times smaller than that of the multigrid setup, and thus the spectral construction does not present a bottleneck. Moreover, both AMG and GEVP are expected to scale roughly as  $\dim Q_h^3$ . However, due to the cubic scaling, the system/preconditioner is unlikely to be assembled/setup in serial. For such a case, a scalable parallel implementation, for the construction of (2.5), remains an issue, and approaches that provide the approximate action of  $H_s$  matrices may offer better performance. Examples of such approaches are the Lanczos method [5, 4], contour integrals [18] or fast Fourier transforms [28]. We refer to [20] for a more thorough discussion of the subject.

**5. Nonmatching discrete trace.** The numerical examples presented thus far have always employed  $\Gamma$ -matching finite element spaces. We note that in [20] this



Table 4.3: Iteration counts and setup costs (in seconds) for system (4.3) and preconditioner (4.4). Both operators are assembled for the complex  $\Gamma$  pictured in Figure 4.1. The number of iterations is bounded in the discretization parameter. In the considered example, the eigenvalue (GEVP) based construction (2.5) does not present a bottleneck as it is 3-4 times cheaper than setting up the algebraic multigrid (AMG).

$\dim V_h$	$\dim Q_h$	#	AMG [s]	GEVP [s]
18K	817	86	0.2	0.1
100K	1605	81	1.9	0.6
634K	3193	76	15.0	4.2
4.8M	6381	68	141.6	36.4

construction is shown to imply that the discrete inf-sup condition holds for problems (4.1) and (2.4) considered with  $\Omega \subset \mathbb{R}^2$  and  $\Gamma$  a one dimensional curve. However, the assumption of matched discretizations of  $\Omega$  and  $\Gamma$  can be too limiting, e.g, if fine resolution is requested on the curve. In this section we present numerical examples using the Babuška problem (4.1), which demonstrate that the assumption is not necessary and to the extent given by the new inf-sup condition the discretizations can be independent. For stable discretizations, preconditioners based on characterization of the trace space will remain optimal. We note that from the point of view of Lemma 3.1 the spaces shall be such that  $V_h|_\Gamma \supset Q_h$ .

**5.1. Codimension 1.** Consider (4.1) with  $\Omega \subset \mathbb{R}^2$ . For  $\Gamma \subset \partial\Omega$ , the finite element discretization of the problem requires that the spaces  $V_h, Q_H$  (we use different subscripts to indicate the difference in underlying triangulations) are such that  $h \leq cH$  for some  $c < 1$ . Here  $h$  is understood as a mesh size of  $V_h$  on  $\Gamma$ . The inequality ensures that the discrete inf-sup condition is satisfied, see, e.g., [34, 12]. We note that [30] shows that the inequality is not necessary.

Let now  $\Gamma$  be a curve, contained in  $\Omega$ , where the domains are discretized such that the condition from the previous paragraph is met. Further, the space  $V_h$  shall be discretized by continuous linear Lagrange elements, while, for the construction of  $Q_H$ , either the same elements or piecewise constant Lagrange elements are employed. We note that with the latter choice the eigenvalue problem for the discrete  $s$ -norm simplifies, since the mass matrix is diagonal in this case.

Table 5.1 reports the number of MINRES iterations on the system (4.1), using  $\text{diag}(\text{AMG}(A + M), H_{-0.5}^{-1})$  as the preconditioner. The iterations are started from a random vector using  $10^{-12}$  as the stopping tolerance for the magnitude of the preconditioned residuum. With both considered finite element discretizations of the multiplier space the number of iterations is bounded indicating (i) that the inf-sup condition is satisfied and (ii) the optimality of the preconditioner. We note that for  $h > H$ , the iterations are unbounded (not reported here) and thus the inf-sup condition is clearly not satisfied. An example of a pair of inf-sup stable and unstable discretizations is shown in Figure 5.1.

**5.2. Codimension 2.** For  $\Gamma$  a manifold of codimension two a condition guaranteeing the discrete inf-sup condition and stability of the discretization of (4.1) is not available. However, we shall assume that the inequality  $h \leq cH$ ,  $c < 1$  plays a role also in the 3d-1d case and discretize the domains accordingly.

The problem (4.1) is considered with two carefully constructed curves  $\Gamma$ , see Figure 5.1, and  $\Omega$  a unit cube discretized such that the inequality is ensured. As

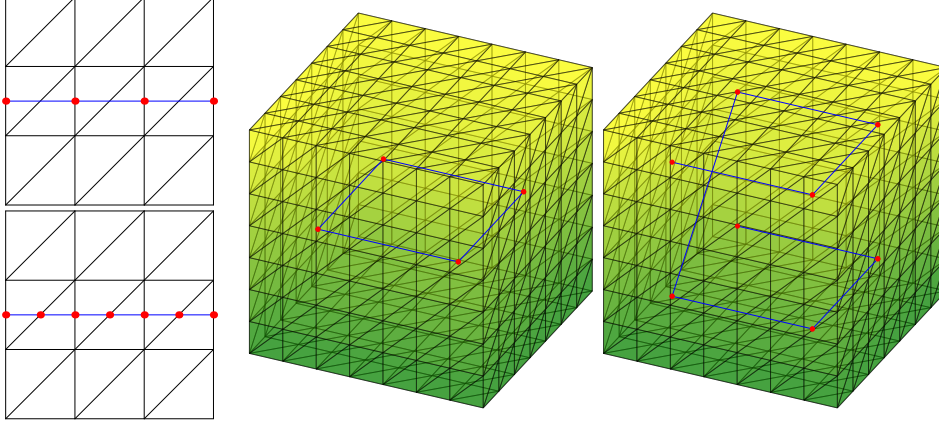


Fig. 5.1: Domains used in experiments with nonmatching discretization. (Left) The spaces  $V_h$  and  $Q_H$  are inf-sup stable for (4.1) if  $h \leq cH$ ,  $c < 1$ . The condition is satisfied/violated in the top/bottom configurations. (Right) The 3d-1d experiments use two curves  $\Gamma$ . The mesh of  $\Omega$  is obtained by first subdividing the domain into odd number of cubes in each direction. Thus degrees of freedom of  $V_h$ ,  $Q_H$  are not associated with identical spatial points. Moreover  $h \ll H$  is ensured in the refinement.

Table 5.1: Iteration counts and error convergence for (4.1) and  $\Omega$  a unit square and  $\Gamma$  a circle. The spaces  $V_h$  and  $Q_H$  are formed either by continuous linear Lagrange elements or  $Q_H$  uses discontinuous piecewise constant Lagrange elements. Note that  $\Gamma$  is closed and thus  $Q_H$  has the same dimension with either of the elements. The inequality  $h \leq cH$ ,  $c < 1$  is respected ensuring that the inf-sup condition is satisfied. Consequently the iteration count is bounded. Both pairs yield optimal, order 1, convergence in  $H^1(\Omega)$  norm of the error  $u - u_h$ . We note that the exact solution is smooth. The error of the Lagrange multiplier measured in the  $s = -\frac{1}{2}$  norm (2.6) (on the same mesh) norm decays with order 1.5.

dim $V_h$	dim $Q_H$	$Q_H$ continuous			$Q_H$ discontinuous		
		#	$\ u - u_h\ _V$	$\ p - p_h\ _Q$	#	$\ u - u_h\ _V$	$\ p - p_h\ _Q$
22K	136	52	9.54E-02	5.28E-03	47	9.54E-02	3.68E-03
87K	272	52	4.78E-02	1.71E-03	48	4.78E-02	1.15E-03
348K	544	51	2.39E-02	5.77E-04	49	2.39E-02	4.18E-04
1.4M	1088	51	1.19E-02	1.87E-04	50	1.19E-02	1.49E-04

before, the spaces  $Q_H$  are constructed from continuous piecewise linear or discontinuous piecewise constant Lagrange elements. We note that the  $\dim Q_h \ll \dim V_h$ . Further, the MINRES iterations use the same initial and convergence conditions as in §5.1, while  $\text{diag}(\text{AMG}(A + M), H_{-0.14}^{-1})$  is used as the preconditioner. In Table 5.2 we observe that the discretization and the preconditioner lead to bounded iteration counts. We note that too fine a discretization of  $\Gamma$ , i.e., violating the inequality, leads to unbounded iterations.

**6. Conclusions.** We have discussed preconditioning of a model multiphysics problem (1.1), where two elliptic subproblems were coupled by a trace constraint, bridging the dimensionality gap of size two. The design of preconditioners for the

Table 5.2: Iteration counts for (4.2) posed on  $\Omega \subset \mathbb{R}^3$  and the two curves pictured in Figure 5.1. For each domain,  $Q_H$  from continuous linear (first column) or discontinuous constant (second column) Lagrange elements is considered. The domains are discretized such that  $h \leq cH$ ,  $c < 1$ . In all the cases, the number of iterations is bounded.

dim $V_h$	Square				Spiral			
	dim $Q_H$	#	dim $Q_H$	#	dim $Q_H$	#	dim $Q_H$	#
33K	16	36	16	24	29	48	28	36
262K	32	38	32	24	57	48	56	35
2.1M	64	36	64	23	113	46	112	35
6.0M	128	38	128	24	225	48	224	36

problem followed our previous work [20]. In particular, the discrete fractional Sobolev norm was employed in order to facilitate the re-use of standard multilevel preconditioners for the 3d domain. Previously, the Sobolev index was dictated by properties of the *continuous* 2d-1d trace operator. Due to the difficulty of establishing a well-posed 3d-1d trace operator for functions in  $H^1$ , we relied on properties of the *discrete* trace. Using spectral and finite element discretizations, a range of suitable (negative) Sobolev indices was found. Consequently, preconditioners for coupled problems were built and their performance was demonstrated by a series of numerical experiments. The proposed preconditioners were robust with respect to the discretization parameter. Finally, the work in [20] was extended by considering independent discretizations of the bulk and embedded domains and by using discontinuous elements for the Lagrange multiplier space.

An obvious weakness of the presented work is the lack of a theoretical foundation, as the well-posedness of (1.1) was assumed and not established. Thus, referring to the idea of operator preconditioning, the continuous picture behind the preconditioner is missing.

**Appendix A. Inf-sup condition for Example 2.1.** Let  $\Omega^- = [0, 1] \times [0, \frac{1}{2}]$ ,  $\Omega^+ = [0, 1] \times [\frac{1}{2}, 1]$ . Further, let  $g \in H_{\frac{1}{2},0}(\Gamma)$  be given. The functions  $u_g^i$ ,  $i \in \{-, +\}$  are the unique weak solutions of  $-\Delta u_g^i = 0$  in  $\Omega^i$  with homogeneous boundary conditions on  $\partial\Omega^i \setminus \Gamma$  and  $Tu_g = g$  on  $\Gamma$ . Then

$$\|u_g^i\|_{H_0^1(\Omega^i)} \leq C_i \|g\|_{H_{\frac{1}{2},0}(\Gamma)}$$

for some constants independent of the domain. Moreover,

$$u_g(x) = \begin{cases} u_g^-(x) & x \in \Omega^- \\ u_g^+(x) & x \in \Omega^+ \end{cases}$$

is such that  $\nabla u_g$  (defined piecewise) is in  $L^2(\Omega)$  and thus  $u_g \in H_0^1(\Omega)$ . Finally, the estimate  $\|u_g\|_{H_0^1(\Omega)} \leq C \|g\|_{H_{\frac{1}{2},0}(\Gamma)}$  holds. Then, by surjectivity of the trace, we get the estimate

$$\begin{aligned} \|q\|_{H_{-\frac{1}{2},0}(\Gamma)} &= \sup_{g \in H_{\frac{1}{2},0}(\Gamma)} \frac{\langle q, g \rangle_{H_{-\frac{1}{2},0}(\Gamma), H_{\frac{1}{2},0}(\Gamma)}}{\|g\|_{H_{\frac{1}{2},0}(\Gamma)}} \leq \frac{1}{C} \sup_{u_g \in H_0^1(\Omega)} \frac{\langle q, Tu_g \rangle_{H_{-\frac{1}{2},0}(\Gamma), H_{\frac{1}{2},0}(\Gamma)}}{\|u_g\|_{H_0^1(\Omega)}} \\ &\leq \frac{1}{C} \sup_{v \in H_0^1(\Omega)} \frac{\langle q, Tv \rangle_{H_{-\frac{1}{2},0}(\Gamma), H_{\frac{1}{2},0}(\Gamma)}}{\|v\|_{H_0^1(\Omega)}} \end{aligned}$$

and the inf-sup condition for (2.7) is satisfied.

**Appendix B. Geometrical configurations and their discretization.** Numerical experiments with the Schur complement in §3.2 and the coupled problem in §4 are considered on sequences of uniformly refined meshes, discretizing the geometrical configurations shown in Figure 4.1. The Schur complement experiment is considered with straight segments  $\Gamma = \{(t, \frac{1}{2}, \frac{1}{2}); t \in [0, 1]\}$  or  $\Gamma = \{(t, t, t); t \in [0, 1]\}$ . For each case the domains are discretized in three ways: (*uniform*) the meshes for  $\Omega$ ,  $\Gamma$  have the same characteristic size, (*finer*) the mesh of  $\Omega$  is finer at  $\Gamma$  than in the rest of the domain, (*coarser*) the mesh of  $\Omega$  is coarser at  $\Gamma$  than in the rest of the domain. Parameters of the meshes for each refinement level are summarized in Table B.1.

Table B.1: Sizes of FEM spaces and mesh parameters for different levels of refinements ( $L$ ). The length of the largest cell in the mesh of  $\Gamma$  is denoted by  $H$ . For readability the reported value is  $H \times 10^3$ . Lengths of smallest/largest edges of cells of the mesh for  $\Omega \setminus \Gamma$  are respectively  $h_{\min}$  and  $h_{\max}$ . (Top) In *uniform* discretization the characteristic mesh size of  $\Omega$  and  $\Gamma$  triangulations are identical. (Middle) *Finer* discretization uses finer mesh near  $\Gamma$ . (Bottom) In the *coarser* cases the mesh of  $\Gamma$  is coarser near the curve.

L	$\Gamma = \{(t, \frac{1}{2}, \frac{1}{2}); t \in [0, 1]\}$					$\Gamma = \{(t, t, t); t \in [0, 1]\}$				
	$\dim V_h$	$\dim Q_H$	$\frac{h_{\min}}{H}$	$\frac{h_{\max}}{H}$	$H$	$\dim V_h$	$\dim Q_H$	$\frac{h_{\min}}{H}$	$\frac{h_{\max}}{H}$	$H$
1	5K	17	1.7	1.7	62.5	5K	17	1.0	1.0	108.3
2	36K	33	1.7	1.7	31.2	36K	33	1.0	1.0	54.1
3	275K	65	1.7	1.7	15.6	275K	65	1.0	1.0	27.1
4	2.1M	129	1.7	1.7	7.8	2.1M	129	1.0	1.0	13.5
5	6.1M	183	1.7	1.7	5.5	6.1M	183	1.0	1.0	9.5
1	12K	161	1.1	32.9	6.2	9K	187	1.0	22.5	9.4
2	72K	321	1.0	35.3	3.1	46K	373	0.9	24.7	4.7
3	476K	641	0.9	39.0	1.6	308K	742	0.8	27.3	2.3
4	3.7M	1281	0.8	40.6	0.8	2.2M	1481	0.8	27.0	1.2
5	6.8M	1601	0.7	40.8	0.6	7.4M	2220	0.8	27.0	0.8
1	11K	9	0.2	1.7	125.0	5K	16	0.2	1.7	122.5
2	59K	17	0.2	1.9	62.5	30K	31	0.2	2.0	61.2
3	375K	33	0.2	2.1	31.2	194K	59	0.2	2.2	30.6
4	2.7M	65	0.2	2.1	15.6	1.4M	114	0.2	2.3	15.5
5	8.5M	97	0.2	2.5	10.4	4.4M	169	0.2	3.2	10.4

## REFERENCES

- [1] R. A. ADAMS AND J. F. FOURNIER, *Sobolev spaces*, vol. 140, Academic press, 2003.
- [2] M. ALNÆS, J. BLECHTA, J. HAKE, A. JOHANSSON, B. KEHLET, A. LOGG, C. RICHARDSON, J. RING, M. ROGNES, AND G. WELLS, *The FEniCS project version 1.5*, Archive of Numerical Software, 3 (2015).
- [3] E. ANDERSON, Z. BAI, C. BISCHOF, S. BLACKFORD, J. DEMMEL, J. DONGARRA, J. DU CROZ, A. GREENBAUM, S. HAMMARLING, A. MCKENNEY, AND D. SORESENSEN, *LAPACK Users' Guide*, Society for Industrial and Applied Mathematics, Philadelphia, PA, third ed., 1999.
- [4] M. ARIOLI, D. KOUROUNIS, AND D. LOGHIN, *Discrete fractional Sobolev norms for domain decomposition preconditioning*, IMA Journal of Numerical Analysis, (2012), p. dr024.
- [5] M. ARIOLI AND D. LOGHIN, *Discrete interpolation norms with applications*, SIAM Journal on Numerical Analysis, 47 (2009), pp. 2924–2951.
- [6] I. BABUŠKA, *The finite element method with Lagrangian multipliers*, Numerische Mathematik, 20 (1973), pp. 179–192.

- [7] C. BACUTA, *A unified approach for Uzawa algorithms*, SIAM Journal on Numerical Analysis, 44 (2006), pp. 2633–2649.
- [8] S. BALAY, J. BROWN, K. BUSCHELMAN, V. EIJKHOUT, W. D. GROPP, D. KAUSHIK, M. G. KNEPLEY, L. C. MCINNES, B. F. SMITH, AND H. ZHANG, *PETSc users manual*, Tech. Report ANL-95/11 - Revision 3.4, Argonne National Laboratory, 2013.
- [9] F. BREZZI, *On the existence, uniqueness and approximation of saddle-point problems arising from Lagrangian multipliers*, Revue française d'automatique, informatique, recherche opérationnelle. Analyse numérique, 8 (1974), pp. 129–151.
- [10] L. CATTANEO AND P. ZUNINO, *A computational model of drug delivery through microcirculation to compare different tumor treatments*, International Journal for Numerical Methods in Biomedical Engineering, 30 (2014), pp. 1347–1371.
- [11] ———, *Computational models for fluid exchange between microcirculation and tissue interstitium*, Networks and Heterogeneous Media, 9 (2014), pp. 135–159.
- [12] W. DAHMEN AND A. KUNOTH, *Appending boundary conditions by Lagrange multipliers: Analysis of the lbb condition*, Numerische Mathematik, 88 (2001), pp. 9–42.
- [13] C. D'ANGELO, *Finite element approximation of elliptic problems with Dirac measure terms in weighted spaces: applications to one-and three-dimensional coupled problems*, SIAM Journal on Numerical Analysis, 50 (2012), pp. 194–215.
- [14] C. D'ANGELO AND A. QUARTERONI, *On the coupling of 1D and 3D diffusion-reaction equations: Application to tissue perfusion problems*, Mathematical Models and Methods in Applied Sciences, 18 (2008), pp. 1481–1504.
- [15] R. D. FALGOUT AND U. MEIER YANG, *hypre: A library of high performance preconditioners*, in Computational Science ICCS 2002, P. M. A. Sloot, A. G. Hoekstra, C. J. K. Tan, and J. J. Dongarra, eds., vol. 2331 of Lecture Notes in Computer Science, Springer Berlin Heidelberg, 2002, pp. 632–641.
- [16] Q. FANG, S. SAKADŽIĆ, L. RUVINSKAYA, A. DEVOR, A. M. DALE, AND D. A. BOAS, *Oxygen advection and diffusion in a three-dimensional vascular anatomical network*, Optics express, 16 (2008), pp. 17530–17541.
- [17] L. GRINBERG, E. CHEEVER, T. ANOR, J. R. MADSEN, AND G. E. KARNIADAKIS, *Modeling blood flow circulation in intracranial arterial networks: a comparative 3D/1D simulation study*, Annals of biomedical engineering, 39 (2011), pp. 297–309.
- [18] N. HALE, N. J. HIGHAM, AND L. N. TREFETHEN, *Computing  $a^\alpha$ ,  $\log A$ , and related matrix functions by contour integrals*, SIAM Journal on Numerical Analysis, 46 (2008), pp. 2505–2523.
- [19] T. KOPPL AND B. WOHLMUTH, *Optimal a priori error estimates for an elliptic problem with Dirac right-hand side*, SIAM Journal on Numerical Analysis, 52 (2014), pp. 1753–1769.
- [20] M. KUCHTA, M. NORDAAS, J. C. G. VERSCHAEVE, M. MORTENSEN, AND K.-A. MARDAL, *Preconditioners for saddle point systems with trace constraints coupling 2d and 1d domains*, SIAM Journal on Scientific Computing, 38 (2016), pp. B962–B987.
- [21] A. A. LINNINGER, I. G. GOULD, T. MARINNAN, C.-Y. HSU, M. CHOJECKI, AND A. ALARAJ, *Cerebral microcirculation and oxygen tension in the human secondary cortex*, Annals of biomedical engineering, 41 (2013), pp. 2264–2284.
- [22] J. L. LIONS AND E. MAGENES, *Non-homogeneous boundary value problems and applications*, vol. 1, Springer Science & Business Media, 2012.
- [23] A. LOGG, K.-A. MARDAL, AND G. WELLS, *Automated solution of differential equations by the finite element method: The FEniCS book*, vol. 84, Springer Science & Business Media, 2012.
- [24] D.S. MALKUS, *Eigenproblems associated with the discrete LBB condition for incompressible finite elements*, International Journal of Engineering Science, 19 (1981), pp. 1299–1310.
- [25] K.-A. MARDAL AND J. B. HAGA, *Block preconditioning of systems of PDEs*, in Automated Solution of Differential Equations by the Finite Element Method, G. N. Wells et al. A. Logg, K.-A. Mardal, ed., Springer, 2012.
- [26] K.-A. MARDAL AND R. WINTHER, *Preconditioning discretizations of systems of partial differential equations*, Numerical Linear Algebra with Applications, 18 (2011), pp. 1–40.
- [27] M. NABIL AND P. ZUNINO, *A computational study of cancer hyperthermia based on vascular magnetic nanoconstructs*, Open Science, 3 (2016).
- [28] P. PEISKER, *On the numerical solution of the first biharmonic equation*, ESAIM: Mathematical Modelling and Numerical Analysis - Modélisation Mathématique et Analyse Numérique, 22 (1988), pp. 655–676.
- [29] J. PESTANA AND A. J. WATHEN, *Natural preconditioning and iterative methods for saddle point systems*, SIAM Review, 57 (2015), pp. 71–91.
- [30] J. PITKÄRANTA, *Boundary subspaces for the finite element method with Lagrange multipliers*,

- Numerische Mathematik, 33 (1979), pp. 273–289.
- [31] J. REICHOLD, M. STAMPANONI, A. L. KELLER, A. BUCK, P. JENNY, AND B. WEBER, *Vascular graph model to simulate the cerebral blood flow in realistic vascular networks*, Journal of Cerebral Blood Flow & Metabolism, 29 (2009), pp. 1429–1443.
  - [32] T. RUSTEN AND R. WINTHER, *A preconditioned iterative method for saddlepoint problems*, SIAM J. Matrix Anal. Appl., 13 (1992), pp. 887–904.
  - [33] D. SILVESTER AND A. WATHEN, *Fast iterative solution of stabilised Stokes systems part ii: using general block preconditioners*, SIAM Journal on Numerical Analysis, 31 (1994), pp. 1352–1367.
  - [34] O. STEINBACH, *Numerical Approximation Methods for Elliptic Boundary Value Problems: Finite and Boundary Elements*, Texts in applied mathematics, Springer New York, 2007.
  - [35] L. N. TREFETHEN AND D. BAU, *Numerical Linear Algebra*, Society for Industrial and Applied Mathematics, 1997.
  - [36] WOLFRAM RESEARCH INC., *Mathematica 8.0*, 2010.

